Dihydroartemisinin ameliorated the inflammatory response and regulated miRNA-mRNA expression profile of chronic nonbacterial prostatitis

Jie Hu[1,A,D], Yan Zhou[2,B], Junhao Wang[2,B], Jianpeng Han[2,B], Jianyong Feng[2,B], Wenbin Chen[2,C], Kuo Guo[2,C], Yongzhang Li[2,A,E,F]

[1] Department of Urology, Langfang People's Hospital, China
[2] Department of Urology, Hebei Province Hospital of Chinese Medicine, Shijiazhuang, China

A – research concept and design; B – collection and/or assembly of data; C – data analysis and interpretation;
D – writing the article; E – critical revision of the article; F – final approval of the article

Advances in Clinical and Experimental Medicine, ISSN 1899–5276 (print), ISSN 2451–2680 (online) *Adv Clin Exp Med*. 2024;33(8):817–829

Address for correspondence
Yongzhang Li
E-mail: liyz@hebcm.edu.cn

Funding sources
This study was funded by the grant from the Natural Science Foundation of Hebei Province (No. H2021423018), Hebei Provincial Health Care Commission (No. 20210302), and Hebei Provincial Administration of Traditional Chinese Medicine (No. 2022040).

Conflict of interest
None declared

Received on March 10, 2023
Reviewed on May 7, 2023
Accepted on September 15, 2023

Published online on November 28, 2023

Abstract

Background. Chronic nonbacterial prostatitis (CNP) is a chronic inflammatory disease. Patients often have trouble urinating, experience painful and frequent urination, and pelvic floor pain, which seriously affects their quality of life. Dihydroartemisinin (DHA) is the most important artemisinin derivative with good anti-inflammatory effects. However, the mechanism of DHA for CNP has not been fully elucidated.

Objectives. To examine the protective effect of DHA on CNP in mice model and to explore the potential mechanisms from the perspective of microRNAs (miRNAs).

Materials and methods. The CNP mouse model was induced using a prostate protein extract solution and complete Freund's adjuvant. The pain threshold was determined using von Frey filaments. Hematoxylin and eosin (H&E) staining, TUNEL staining, western blot, real-time polymerase chain reaction (PCR), and small RNA sequencing were used to evaluate the effect of DHA on CNP.

Results. Dihydroartemisinin significantly alleviated prostate tissue damage in CNP mice, reduced the pain threshold, improved the prostate index, and reduced cell apoptosis. It also reduced the expressions of interleukin-1β (IL-1β), interleukin-6 (IL-6), tumor necrosis factor-α (TNF-α), and macrophage chemoattractant protein-1 (MCP-1). Furthermore, after screening 48 differentially expressed genes, we found 4 miRNAs significantly downregulated and 2 miRNAs upregulated in the model group, which were later significantly reversed by DHA treatment. These results indicate that DHA treatment of CNP involves several signaling pathways.

Conclusions. Dihydroartemisinin can improve the pathological state and inflammatory response in a CNP mouse model, which may be related to the regulation of miRNAs.

Key words: inflammation, dihydroartemisinin, chronic nonbacterial prostatitis, small RNA sequencing

Cite as
Hu J, Zhou Y, Wang J, et al. Dihydroartemisinin ameliorated the inflammatory response and regulated miRNA-mRNA expression profile of chronic nonbacterial prostatitis. *Adv Clin Exp Med*. 2024;33(8):817–829. doi:10.17219/acem/172386

DOI
10.17219/acem/172386

Background

Chronic prostatitis is a chronic inflammation that affects approx. 8–11.5% of men worldwide,[1,2] and more than 90% of chronic prostatitis are caused by chronic nonbacterial prostatitis (CNP).[3,4] Patients often experience difficulty urinating, painful and frequent urination, and pelvic floor pain, which seriously affects their quality of life.[5] Due to the multifactorial and complex pathogenesis of CNP, its mechanism has long been debated. However, at present, it remains not fully elucidated. Most researchers believe it is caused by a combination of etiological infection, inflammation, abnormal neuromuscular activity in the pelvic floor, and immune abnormalities.[6] Notably, inflammation plays a key role in the pathogenesis of many diseases.[7–10] Antibiotics, botanicals, alpha-blockers, and non-steroidal anti-inflammatory analgesics are common treatment methods for CNP.[11] However, chemicals are not appropriate as permanent therapeutics because they are prone to adverse reactions. Antibiotics are unlikely to help unless combined with alpha-blockers, and they are prone to dependence.[12] Surprisingly, the therapeutic role of traditional Chinese medicine (TCM) and some botanical ingredients in the treatment of chronic prostatitis has received increasing attention in recent years.[13,14] Therefore, the search for a safe, efficient and well-absorbed botanical component is of great importance for the treatment of CNP.

Recently, there has been remarkable advancement in TCM research. Some natural products have significant anti-inflammatory activity and promising applications for treating prostate diseases. Artemisinin is a special sesquiterpene lactone containing a peroxide bond extracted from the annual Compositae family member *Artemisia annua* L., which is an effective antimalarial component.[15,16] Dihydroartemisinin (DHA) is the most important artemisinin derivative, created by the oxidation of artemisinin with sodium tetrahydroborate.[17] As the first-generation derivative of artemisinin, DHA has better water solubility and stability, high efficiency, low toxicity, and strong activity.[18] In recent years, some studies have confirmed that DHA has anti-inflammatory, anti-tumor, antibacterial, and immunomodulatory characteristics, in addition to antimalarial properties.[15,19–21] Moreover, studies have reported that DHA improved the symptoms of systemic lupus erythematosus in mice and regulated the secretion of the pro-inflammatory mediator tumor necrosis factor-α (TNF-α). It was thought that the possible mechanism was via the inhibition of NF-κB-induced inflammatory cascade by affecting NF-κB activation and translocation to the nucleus.[22] Previously, we investigated the protective effect of DHA on hyperglycemia-induced vascular smooth muscle cell (VSMC) proliferation and associated inflammation. Dihydroartemisinin dramatically lowered the mRNA levels of interleukin-1β (IL-1β) and TNF-α, and this mechanism may play a protective role in VSMC proliferation and inflammation via suppressing the *miR-376b-3p/KLF15* axis.[23] Previous research has demonstrated that DHA can lower the generation of inflammatory factors in prostatitis tissues and alleviate prostatitis and the inflammatory response by inhibiting the E2F7/HIF1α pathway.[24]

However, little attention has been paid to gene regulation. MicroRNAs (miRNAs) have been extensively studied in many diseases, and their expression can be modulated by many different compounds.[25] To identify CNP-specific differentially expressed miRNAs (DEMs) and mRNAs, we used a bioinformatics approach to investigate candidate miRNA-mRNA expression profiles of DHA involved in the CNP pathogenesis.

Objectives

In this study, we investigated the therapeutic impact of DHA on CNP mice from pharmacogenetic point of view and examined the underlying mechanisms responsible for this effect. The effect of DHA on miRNA-mRNA expression profile in the prostate tissue of CNP model mice was investigated by small RNA sequencing, which laid the foundation for the study on CNP.

Materials and methods

Animal experiments

Animals and drugs

Male nonobese diabetic (NOD) mice (6–8 weeks old, 20–22 g), supplied from Beijing Zhongke Zesheng Biotechnology Co., Ltd. (Beijing, China), were used in all experiments. Before experimental manipulation, all animals were exposed to 12 h of light and dark cycle and constantly supplied with food and drink for at least 7 days. The mice were fed a general experimental animal diet provided by Chengdu Dossy Experimental Animal Co., Ltd. (Chengdu, China). The composition of the animal diet was as follows: corn, soybeans, bone flour, wheat, fish flour, sodium chloride, and vitamin complex. All animal procedures were approved by the Laboratory Animal Ethical and Welfare Committee of Hebei Medical University (approval No. IACUC-Hebmu-P2021075). Dihydroartemisinin was purchased from Shanghai Yuanye Biotechnology Co., Ltd (batch No. B21182, purity ≥98%).

Experimental autoimmune prostatitis

Prostate tissue was harvested from Sprague–Dawley rats under aseptic conditions, washed with saline, and added to a saline solution containing 0.5% Triton X-100. The prostate tissue was homogenized on ice prior to centrifugation to obtain the supernatant. The bicinchoninic acid (BCA)

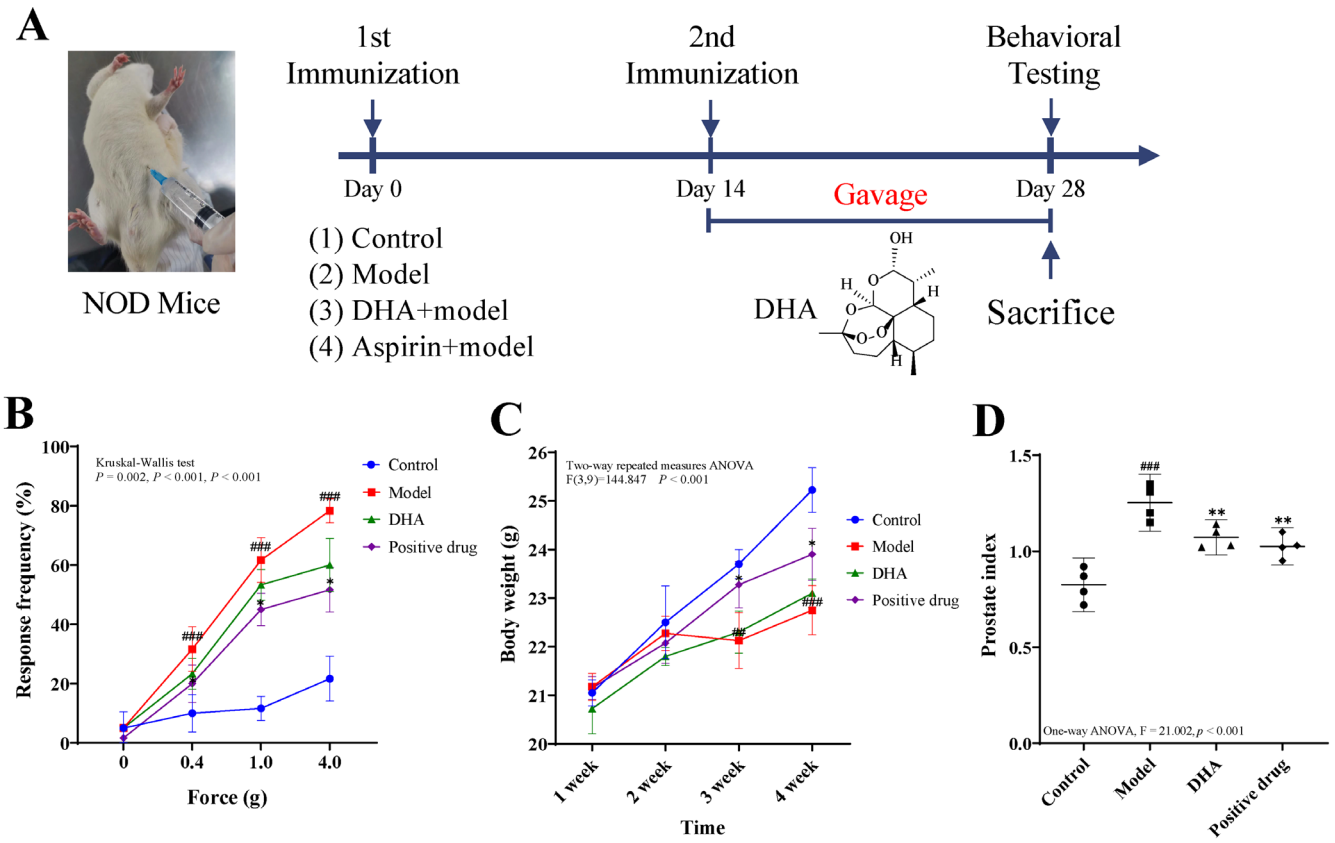

Fig. 1. Dihydroartemisinin improved nociceptive sensitivity in chronic nonbacterial prostatitis (CNP) mice. A. The experimental method is depicted in a timeline diagram; B. Nonobese diabetic (NOD) mice responded to mechanical abdominal stimulation using von Frey filaments at forces of 0, 0.4, 1.0, and 4.0 g. Response frequency was analyzed by the Kruskal–Wallis test (n = 6); C. Body weight changes of mice; p-value calculated for the difference between groups by two-way repeated measures analysis of variance (ANOVA) (n = 6); D. DHA significantly decreased the prostate index compared with the model group. The prostate index was analyzed by one-way ANOVA (n = 4). Data are presented as the means and 95% confidence interval (95% CI) whiskers

$^{\#\#}p < 0.01$; $^{\#\#\#}p < 0.001$ vs control group; $^{*}p < 0.05$; $^{**}p < 0.01$ compared with the model group; DHA – dihydroartemisinin group.

protein concentration assay kit was used to determine the protein concentration in the supernatant, which was adjusted to 20 mg/mL. Subsequently, the rat prostate protein purification solution was combined with an equivalent volume of complete Freund's adjuvant via ultrasound to make a suspension.

Nonobese diabetic mice (n = 24) were randomized into control, model, DHA (150 mg/kg), and positive drug (aspirin tablets, 150 mg/kg) groups (n = 6). Each mouse in the control group was injected subcutaneously with phosphate buffer saline (PBS) + complete Freund's adjuvant (0.1 mL). In the experimental autoimmune prostatitis (EAP) model group, DHA group and positive drug group, each mouse was injected subcutaneously with 0.1 mL of purified prostate protein solution and complete Freund's adjuvant. A second immunization was performed after 14 days to establish a mouse model of chronic nonbacterial prostatitis, EAP. The DHA and positive drug groups were administered by gavage starting with the second immunization and repeated every 2 weeks until 28 days of harvesting. The pain thresholds were measured using von Frey fiber filaments on day 28. All mice were sedated with ip. pentobarbital (5%, 50 mg/kg), and the prostate tissue was immediately isolated and weighed to calculate the prostate index. Prostate index = prostate weight (mg)/body weight (g). The tissues were stored in a −80°C environment for later analysis. The detailed experimental procedure is shown in Fig. 1A.

Behavioral nociception measurement

The pain threshold of NOD mice was determined using von Frey filaments, and the skin abnormalities were assessed on day 28 after immunization.[26] The test was performed in a transparent plastic chamber with a stainless-steel grid floor. Mice were placed in the experimental room for at least 30 min to acclimatize to the environment before the behavioral tests began. Von Frey filaments were then used to measure the tactile abnormal discomfort and hyperalgesia in each mouse at forces of 0, 0.4, 1.0, and 4.0 g, respectively. Von Frey filaments were administered on the abdomen for 1–2 s, 10 times, with 2 min between each stimulation. To prevent desensitization, stimulation was limited to the lower abdomen and varied areas within this area were stimulated. Positive reactions to filament stimulation were classified into 3 types, namely 1) abrupt abdominal retraction; 2) quick

licking or scratching; or 3) jumping.[27] The percentage reaction frequency was calculated as [(the number of positive responses/10 trials) × 100 = percentage response frequency].

Hematoxylin and eosin staining

The prostate tissue was fixed, dehydrated and embedded in paraffin before being cut into sections and stained as follows.[28] The prostate tissue sections were first dewaxed, and then stained with hematoxylin for 20 min. Next, after being separated by HCl/95% alcohol for 10 s, they were put into a weak ammonia solution at 50°C to return to a blue color. The slides were then stained with eosin for 5 min. Sections then underwent a soaking process in graded concentrations of alcohol, followed by treatment with xylene to achieve transparency. They were then sealed with neutral gum and examined under a microscope (Zeiss AxioVision, Oberkochen, Germany).

TUNEL staining

TUNEL staining was performed in the previous study.[29] To prepare the tissue sections, they were first deparaffinized and rehydrated, and then soaked in water for 5 min. Antigen retrieval was performed with a microwave, heating the samples for 8 min, followed by 3 washes with PBS (5 min per wash). Next, a TUNEL reaction mixture consisting of 50 µL TDT and 450 µL fluorescein-labeled dUTP solution was added to each slice, which was then incubated at 37°C for 1 h. Then, the sections were rinsed with PBS for 5 min × 3 times. DAPI nuclear staining was performed for 5 min, followed by rinsing with PBS and mounting the sections with 50% glycerol. The samples were stored at –20°C for microscopic examination (Nikon, Tokyo, Japan). The TUNEL analysis was assessed as 10 visual fields per mouse, and the apoptosis rate of each mouse was calculated.

Western blotting

The tissues were first frozen and subsequently ground to a powder. The resulting powder was then lysed using RIPA lysate while kept on ice for 15 min. The lysed samples were then centrifuged at 12,000 rpm at 4°C for 10 min, and the resulting supernatant was collected. The protein concentration of the supernatant was determined using a BCA protein assay kit. To denature proteins, they were heated at 95°C for 5 min before being stored at a low temperature (–80°C) for subsequent analysis. Next, the samples were separated on 8–10% sodium dodecyl-sulfate polyacrylamide gel electrophoresis (SDS-PAGE) gels and transferred onto polyvinylidene fluoride (PVDF) membranes (Millipore, Billerica, USA). The membranes were blocked with 5% skim milk and left in a shaker for 2 h at 37°C. Then, primary antibodies (anti-IL-1β, No. A1112, 1:2000; anti-IL-6, No. A0286, 1:2000; anti-TNF-α, No. A11534, 1:2000; MCP-1, No. A22744, 1:2000; β-actin, No. AC026, 1:100,000; all from Abclonal, Woburn, USA) were added and incubated overnight at 4°C. After washing with PBS, they were incubated with secondary antibodies (goat anti-rabbit IgG (H + L), No. s0001, 1:5000; Affinity, Changzhou, China) for 2 h, then washed with Tris-buffered saline with Tween (TBST) 3 times and colored by enhanced chemiluminescence (ECL) (Bio-Rad, Foster City, USA). Finally, the images were scanned and analyzed by a gel image analysis system.

Small RNA sequencing

The total RNA extraction reagent Trizol was used to obtain the total RNA. An Agilent Bioanalyzer 2100 (Agilent Technologies, Santa Clara, USA) was used to evaluate sample concentration and integrity, which served as a reference for the library building and bioinformatic analysis. Polyacrylamide gel electrophoresis (PAGE) was used to separate the RNA fragments, and short RNAs with lengths of 18–30 nt were obtained. The Illumina TruSeq Small RNA Sample Prep kit (New England Biolabs, Inc., Ipswich, USA) was used to create small RNA libraries. Then, enriched libraries were amplified by polymerase chain reaction (PCR) to enrich cDNA with both 3' and 5' connectors. After cDNA amplification, the small RNA libraries were further purified by electrophoresis. The quality of the library was identified using an Agilent 2100 Bioanalyzer and an Agilent High Sensitivity DNA Kit (Agilent Technologies, Foster City, USA), with the criterion of the qualified libraries showing only a single peak and no junction. The libraries were then measured using the Quan-iT PicoGreen dsDNA assay kit (Thermo Fisher Scientific, Waltham, USA), and the Illumina platform was used for RNA sequencing. Single-stranded cDNA was used as a template for PCR amplification and sequencing by annealing a sequencing primer. The target genes of these miRNAs were classified after the identification of DEMs using sequencing. Finally, the miRNA targets were subjected to Gene Ontology (GO) and Kyoto Encyclopedia of Genes and Genomes (KEGG) pathway analyses.

miRNA qPCR analysis

Total RNA was extracted using the Molpure® cell/tissue total RNA kit (No. 19221ES50; Yeasen Biotechnology Co., Ltd., Shanghai, China) according to the manufacturer's instructions. Reverse transcription (RT) reactions were performed using Bulge-LoopTM miRNA RT primers (No. R10031.7; RiboBio, Guangzhou, China) and Bulge-Loop™ miRNA qRT-PCR starter kit (No. R11067.2; RiboBio). The RT reaction procedure was performed at 42°C for 60 min and at 70°C for 10 min. Real-time PCR reactions were performed using 2X SYBR Green Mix, Bulge-Loop™ miRNA Forward Primer, and Bulge-Loop™ Reverse Primer. The reaction conditions

were as follows; pre-denaturation, 95°C, 10 min; denaturation, 95°C, 2 s; annealing, 60°C, 2 s; extension, 70°C, 10 s. All data were analyzed by a QuantStudio TM3 instrument (Thermo Fisher Scientific).

Data analysis and statistical methods

GraphPad Prism 8.0 (GraphPad Software, San Diego, USA) and IBM SPSS 25.0 statistical software (IBM SPSS, Armonk, USA) were used for statistical analysis. The Shapiro–Wilk method was first used to test for normal distribution, and these were expressed as mean ± standard deviation (SD), and non-normally distributed data were expressed as median and percentiles (25^{th} percentile (P25) and 75^{th} percentile (P75)). For data obeying normal distribution, one-way ANOVA was used for comparison between multiple groups, Levene's test was used for homogeneity of variance analysis, the LSD test for data with homogeneity of variance, and Tamhane's T2 test for data with unequal variance. Repeated measures were analyzed using a two-way repeated measures ANOVA followed by Bonferroni's multiple comparison test. Comparisons of non-normally distributed data were analyzed by nonparametric tests using the Kruskal–Wallis method. All data are presented as the means and 95% confidence interval whiskers. The value of $p < 0.05$ was considered statistically significant. In addition, Spearman's correlation analysis was utilized to compare 2 genes, with $p < 0.05$ representing statistical significance.

Results

DHA improved nociceptive sensitivity in the CNP model mice

The pain threshold of NOD mice was evaluated by von Frey filaments on day 28 after immunization to evaluate the effect of DHA on chronic pelvic pain in the CNP mice. The response frequency to tactile hypersensitivity was considerably greater in the model group compared with the control group (Kruskal–Wallis, $F = 20.205$, $p < 0.001$), and the response frequency was higher after the second vaccination compared to the first, indicating that CNP can directly produce pain in mice. The response frequency was lower in the DHA and positive drug groups compared with the model group under the forces of 0.4 g, 1.0 g and 4.0 g, respectively (Fig. 1B, Supplementary Table 1). To varying degrees, continuous daily doses of DHA and aspirin reduced the frequency of CNP-induced responses, suggesting that DHA has a pain-relieving effect on CNP mice.

Four weeks later, the average body weight of mice treated with rat prostate protein + Freund's adjuvant decreased sharply ($F (3.9) = 144.847$, $p < 0.001$). However, body weight increased after DHA administration, although it remained significantly lower than in the control group (Fig. 1C, Supplementary Table 1). We also investigated how DHA affected benign prostatic hyperplasia (BPH). The prostate index, which is the ratio of prostate weight to body weight, can be used to indicate BPH. Our results revealed that the prostate index was raised in the model group (one-way ANOVA, $F = 21.002$, $p < 0.001$) but was lowered by DHA treatment (one-way ANOVA, $F = 21.002$, $p = 0.006$) (Fig. 1D, Supplementary Table 1). The difference in prostate index between the DHA and model group may be due to DHA reducing the inflammatory congestion and edema of the prostate tissue in mice.

DHA ameliorated histopathological damage and apoptosis of prostate tissue in the CNP model mice

Next, we evaluated the effect of DHA on prostate tissue using pathological staining. Hematoxylin and eosin staining of prostate tissues showed that the control group contained normal structures without histopathological changes. The prostate tissue framework in the control group was integrated and transparent and exhibited an enlarged gland cavity with many folds. Moreover, the prostate gland exhibited a monolayer of flattened, cuboidal, columnar, or pseudostratified columnar glandular epithelium, which was neatly arranged and without showing obvious degeneration and necrosis. The model group's prostate tissue structure was considerably deteriorated as compared to the control group. It was obvious that some of the glandular ducts in the tissue were obscured, epithelial cells displayed degeneration and necrosis, were relatively flat with surrounding interstitial edema and inflammatory cell infiltration, and a large number of lymphocytes were observed. Surprisingly, the prostate tissue improved markedly after DHA therapy. However, edema with inflammatory cell infiltration, lymphocytes, plasma cells, neutrophils and mast cells could still be observed in the interstitium surrounding the glandular duct (Fig. 2A).

The principle of the TUNEL technique is that apoptosis is detected by labeling the 3'-OH site of DNA with fluorescein-conjugated nucleotides in the presence of deoxyribonuclease (TdT). Nuclei were stained with DAPI, and yellow cells were considered apoptotic. The results of TUNEL staining showed that DHA ameliorated cell apoptosis in the prostate tissue (Fig. 2B). Freund's adjuvant stimulation significantly increased apoptosis in prostate cells (one-way ANOVA, $F = 271.622$, $p < 0.001$), although the significant increase of apoptosis level in the model group was suppressed by DHA (one-way ANOVA, $F = 271.622$, $p < 0.001$) (Fig. 2C, Supplementary Table 2).

DHA reduced inflammatory factors of prostate tissue in the CNP model mice

We used western blot analysis to identify the expression of numerous common inflammatory markers, including

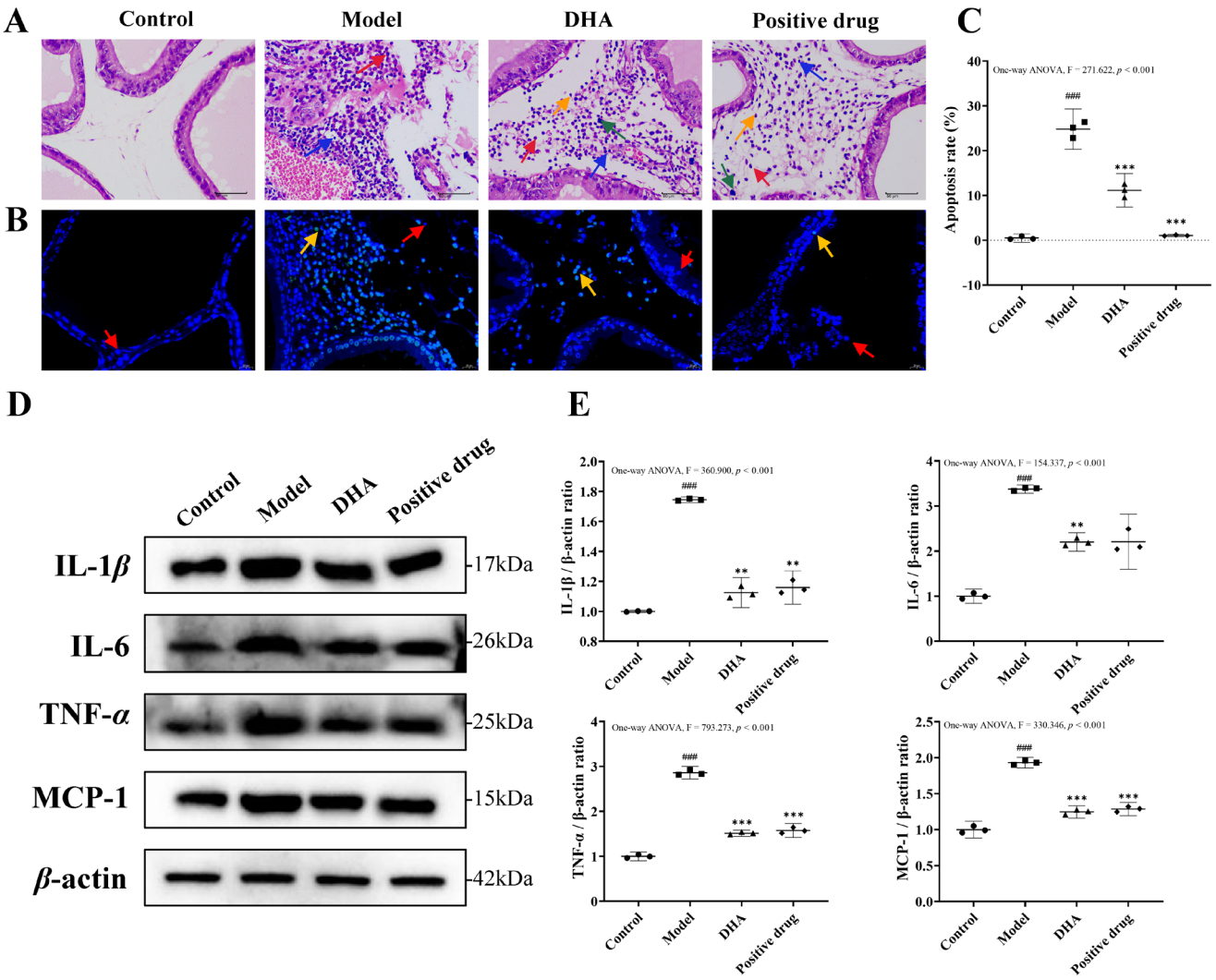

Fig. 2. Dihydroartemisinin ameliorated histopathological damage, apoptosis and inflammatory response in prostate tissue of chronic nonbacterial prostatitis (CNP) mice. A. Hematoxylin and eosin (H&E) staining of prostate tissues. All images are exhibited at the same magnification, ×400, scale bar = 50 μm; B. Representative TUNEL images show that DHA ameliorated apoptosis in prostate cells. Blue represents nuclear staining (red arrow), and green represents TUNEL staining (yellow arrow), scale bar = 20 μm; C. The apoptosis rate of prostate cells; D. The protein expression of IL-1β, IL-6, TNF-α, and MCP-1 in the prostate tissues was detected using western blotting; E. Densitometric analysis of IL-1β, IL-6, TNF-α, and MCP-1 protein expression normalized to β-actin content (n = 3). Data are presented as the means and 95% confidence interval (95% CI) whiskers. Statistical analysis of the data was performed using one-way analysis of variance (ANOVA)

###p < 0.001compared with the control group; **p < 0.01; ***p < 0.001compared with the model group; DHA – dihydroartemisinin group.

IL-1β, interleukin-6 (IL-6), TNF-α, and macrophage chemoattractant protein-1 (MCP-1), in prostate tissues to better understand how DHA inhibits CNP by reducing inflammation. According to the findings, IL-1β, IL-6, TNF-α, and MCP-1 levels in the CNP mice were significantly elevated ($F = 360.900$, $p < 0.001$; $F = 154.337$, $p < 0.001$; $F = 793.273$, $p < 0.001$; $F = 330.346$, $p < 0.001$), whereas DHA dramatically decreased these proteins' expression ($F = 360.900$, $p = 0.006$; $F = 154.337$, $p = 0.002$; $F = 793.273$, $p < 0.001$; $F = 330.346$, $p < 0.001$) (Fig. 2D,E, Supplementary Table 2). Overall, these findings displayed that DHA could attenuate CNP and antagonize the inflammatory response.

DHA affected the miRNA-mRNA expression profile of prostate tissue in the CNP mouse model

Data filtering and small RNA sorting

Small RNA sequencing was performed on the control group, model group and DHA group, producing a total of 201,337,093 raw reads and 197,003,650 clean reads (≥18 nt) from 9 samples (3 samples per group). We discarded sequences with average sequencing quality below 20 and then filtered them for subsequent analysis. The average clean rate was 97.83%, which indicated that the quality control of sequencing data was reliable (Table 1). We then summarized the annotation of all small RNAs compared to various types of RNAs (Fig. 3A).

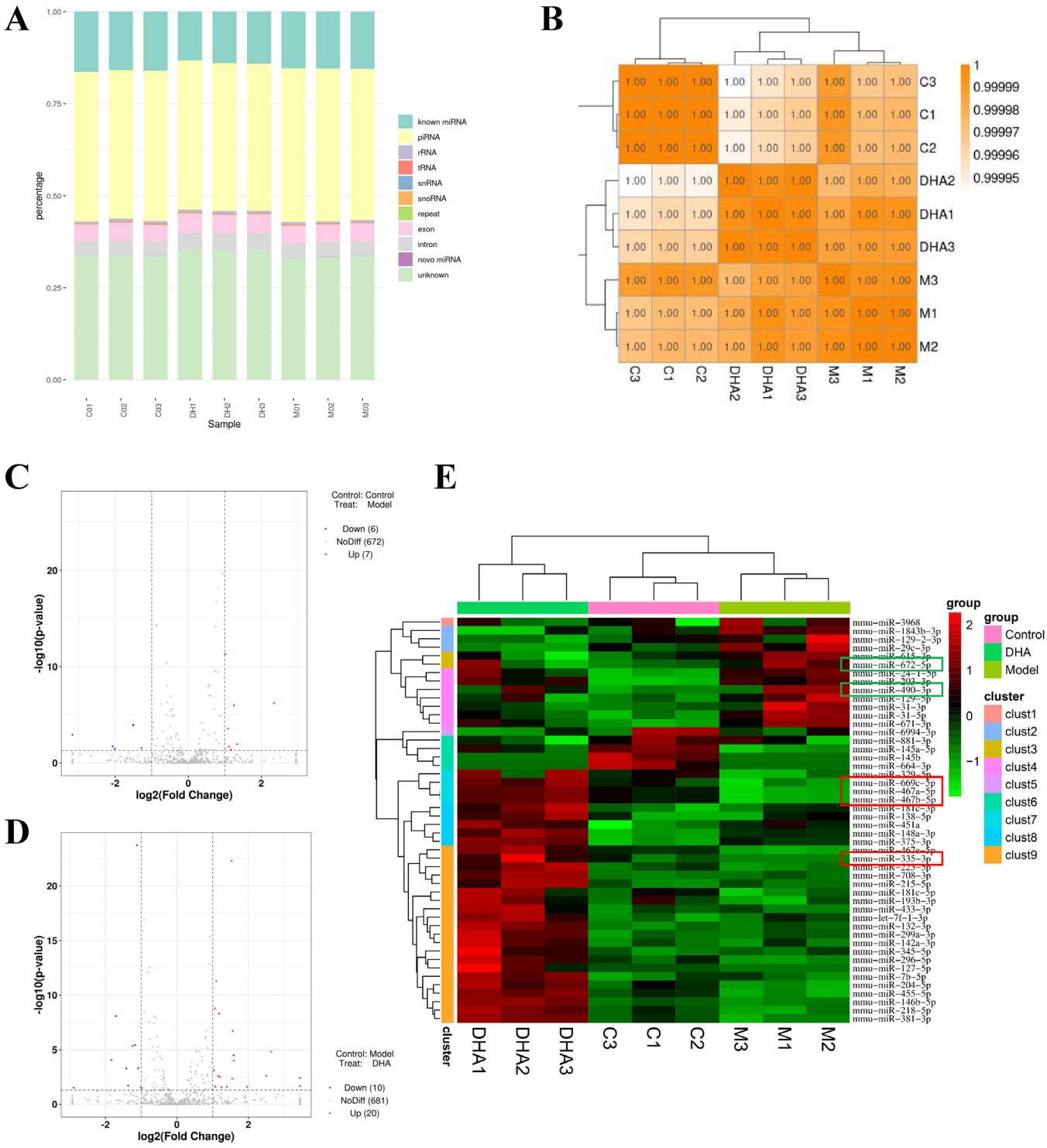

Fig. 3. Dihydroartemisinin affected miRNA-mRNA expression profile of prostate tissue in the chronic nonbacterial prostatitis (CNP) mice. A. Small RNA classification statistics chart. The horizontal coordinate is the sample name, and the vertical coordinate is the proportion of de-duplicated sequences annotated to various RNAs to the total de-duplicated sequences; B. Pearson correlation coefficient for a sample test. The left and the top are the sample clustering cases, the right and the bottom are the sample names, and the squares of different colors represent the high or low correlation between the 2 samples. Volcano map of differentially expressed genes (DEGs) in the control vs model group (C) and the model vs DHA group (D). Red dots represent upregulated genes, blue dots represent downregulated genes, and gray dots represent non-significant DEGs (fold change ≥2, $p \leq 0.05$); E. Heatmap of DEMs in each sample based on hierarchical clustering analysis. The distance was calculated using the Euclidean method, and hierarchical clustering was applied. MiRNA with the most similar expression patterns are grouped together. Clustering was accomplished through the usage of complete linkage. Green denotes low expression, whereas red denotes strong expression

C – control group; M – model group; DHA – dihydroartemisinin group.

Table 1. Sequencing data volume statistics for 9 samples

Sample	Raw reads	Clean reads	Clean rate (%)
C1	22, 999, 745	22, 549, 376	98.04
C2	24, 645, 074	24, 130, 473	97.91
C3	23, 197, 912	22, 677, 066	97.75
DHA1	19, 053, 157	18, 560, 325	97.41
DHA2	18, 479, 443	18, 042, 214	97.63
DHA3	21, 294, 151	20, 808, 361	97.72
M1	22, 018, 657	21, 606, 038	98.13
M2	24, 522, 043	23, 972, 182	97.76
M3	25, 126, 911	24, 657, 615	98.13

Clean reads (≥18 nt) – number of filtered sequences (nucleotide length ≥18 nt); C – control group; M – model group; DHA – dihydroartemisinin group.

Screening and analysis of differentially expressed miRNAs

We conducted a Pearson correlation coefficient analysis to find any correlation between miRNA expressions (Fig. 3B). The Pearson correlation coefficient was 0.99, indicating that the samples were extremely strongly correlated with each other. Next, we analyzed the differences in miRNA expression levels by DESeq (the criteria are based on |log2(fold-change)| ≥1 and $p < 0.05$). The findings revealed that 13 miRNAs were significantly modified in the model group ($p < 0.05$), with 7 miRNAs upregulated and 6 miRNAs downregulated (Fig. 3C). A total of 30 miRNAs were notably expressed in the DHA group ($p < 0.05$), with 20 miRNAs being upregulated and 10 miRNAs being downregulated (Fig. 3D). Next, we performed bidirectional clustering analysis of all miRNAs and samples, which revealed differences in 48 differentially expressed genes in each sample (Fig. 3E). Four miRNAs (*miR-467a-5p*, *miR-467b-5p*, *miR-335-3p*, *miR-669c-5p*) were downregulated in the CNP mice and upregulated after DHA treatment, while 2 miRNAs (*miR-490-3p*, *miR-672-5p*) were upregulated in the CNP mice and downregulated after DHA treatment (Table 2). Subsequently, we detected 6 differentially expressed miRNAs in prostatitis tissues using real-time quantitative PCR (Fig. 4A–F, Supplementary Table 3), and statistical analysis was performed using one-way ANOVA and Kruskal–Wallis test. Although there was no significant difference in the expression of *miR-669c-5p* (one-way ANOVA, $F = 12.930$, $p = 0.134$), *miR-467a-5p*, *miR-467b-5p* and *miR-335-3p* displayed reduced expression in the model group compared to the control group ($F = 6.006$, $p = 0.017$; $F = 25.987$, $p < 0.001$; $F = 6.030$, $p = 0.015$), and the expression levels of *miR-467b-5p* and

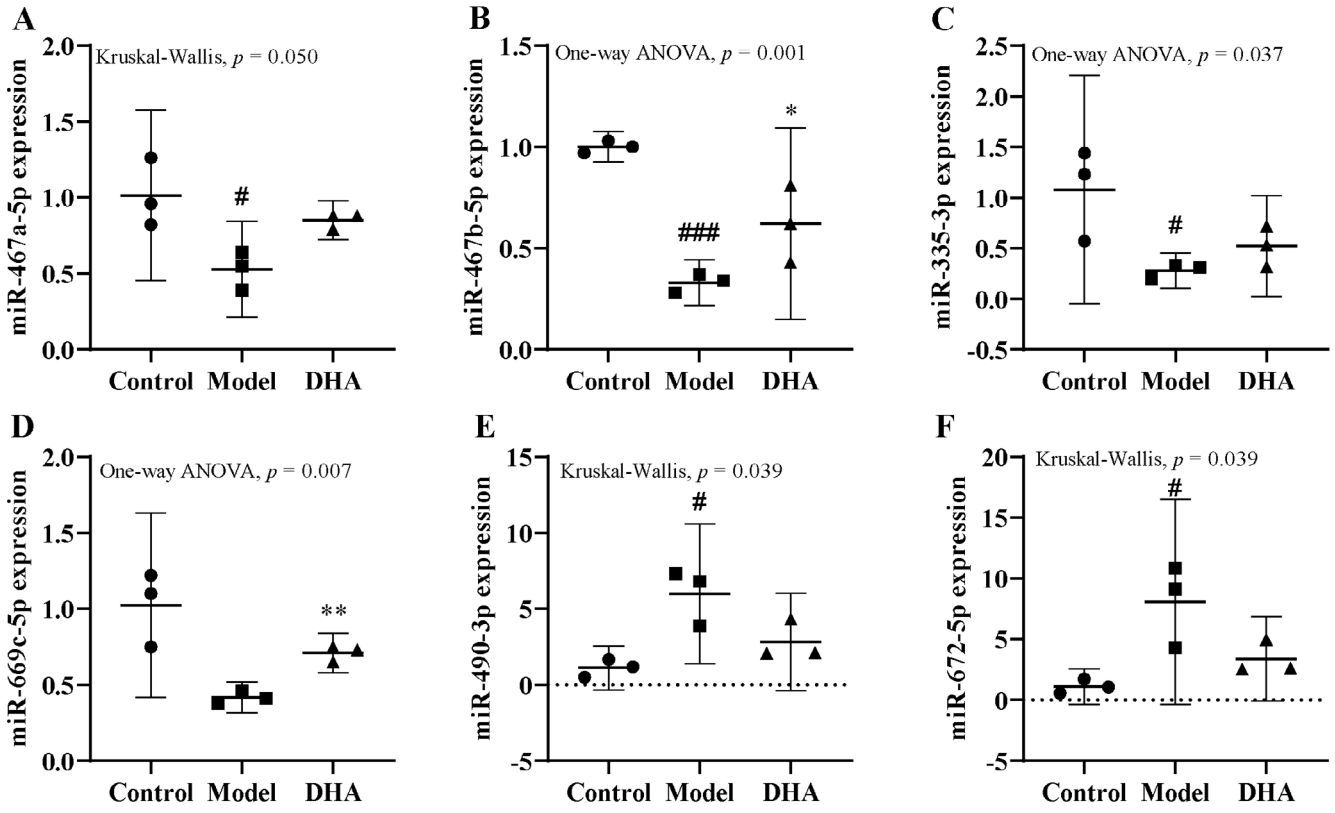

Fig. 4. Identification of 6 differentially expressed miRNAs in prostatitis tissues. The expressions of *miR-467a-5p* (A), *miR-467b-5p* (B), *miR-335-3p* (C), *miR-669c-5p* (D), *miR-490-3p* (E), and *miR-672-5p* (F) in prostatitis tissues were detected using real-time quantitative polymerase chain reaction (PCR) (n = 3). Data are presented as the means and 95% confidence interval (95% CI) whiskers. Statistical analysis of the data was performed using one-way analysis of variance (ANOVA) and Kruskal–Wallis test

$^{\#}p < 0.05$; $^{\#\#\#}p < 0.001$ compared with the control group; $^{*}p < 0.05$; $^{**}p < 0.01$ compared with the model group; DHA – dihydroartemisinin group.

Table 2. Differentially expressed miRNAs responding to dihydroartemisinin (DHA) treatment

miRNA	FoldChange (model/control)	log2FoldChange	p-value	Regulate	FoldChange (DHA/model)	log2FoldChange	p-value	Regulate
miR-467a-5p	0.353	–1.504	1.147E–04	down	3.006	1.588	3.204E–05	up
miR-467b-5p	0.353	–1.504	1.147E–04	down	3.006	1.588	3.204E–05	up
miR-335-3p	0.248	–2.014	3.394E–02	down	5.646	2.497	2.418E–03	up
miR-669c-5p	0.412	–1.278	2.889E–02	down	2.937	1.554	4.501E–03	up
miR-490-3p	2.381	1.252	1.011E–06	up	0.445	–1.169	3.630E–06	down
miR-672-5p	2.257	1.174	4.113E–02	up	0.389	–1.363	1.936E–02	down

FoldChange represents the differential multiples of gene expression between the control group and the model group, or the model group and the DHA group; $p < 0.05$.

miR-669c-5p were higher after DHA treatment compared to the model group before treatment ($F = 25.987$, $p = 0.021$; $F = 12.930$, $p = 0.006$). In contrast, *miR-490-3p* and *miR-672-5p* levels were higher in the model group when compared to the control group ($F = 6.489$, $p = 0.011$; $F = 6.489$, $p = 0.011$), while *miR-490-3p* and *miR-672-5p* levels were lower in the DHA group relative to the model group. However, this final result did not reach statistical significance, which was consistent with the sequencing data.

miRNA target gene prediction and bioinformatics analysis

We performed target gene prediction on differentially expressed miRNA sequences. A total of 48 miRNAs were analyzed, resulting in 15,689 predicted target genes, and 73,083 predicted target sites. To investigate the function and mechanisms of miRNA target genes, GO and KEGG pathway enrichment studies were carried out. Gene Ontology enrichment analysis of the control compareed to the model group showed that there were 1887 statistically significant GO term entries in the total differential genome ($p < 0.05$). The top 20 enriched GO terms of control vs model groups are shown in Fig. 5A. The biological processing (BP) contained "regulation of cellular process", "regulation of biological process", "signaling", etc. For the cellular components (CC), terms related to "membrane" and "cell periphery" were enriched, while the molecular function (MF) included olfactory receptor activity. In the control vs model group, there were 2,631 statistically significant GO term entries in the total differential genome ($p < 0.05$). The top 20 enriched GO terms of model vs DHA groups were involved in BP (cellular process, biological regulation, regulation biological process, regulation of the cellular process, etc.) and CC (cell periphery, membrane, intracellular, etc.) (Fig. 5B).

Further KEGG pathway analysis of the control vs model group showed that 27 pathways were enriched ($p < 0.05$), including 5 major categories, namely "organismal systems", "human diseases", "environmental information processing", "cellular processes", and "metabolism". Correspondingly, pathways were also involved in cancer (breast cancer, microRNAs in cancer), glycan biosynthesis and metabolism, signal transduction (phosphatidylinositol signaling system, Wnt, MAPK, Rap1, and sphingolipid signaling pathway), lipid metabolism (biosynthesis of unsaturated fatty acids), and infectious disease: bacterial (yersinia infection), among others. Detailed information is shown in Fig. 5C. In the model vs DHA group, there were 94 statistically significant KEGG pathways in the total differential genome ($p < 0.05$). The top 20 signaling pathways were divided into 4 major categories, "cellular processes", "human diseases", "organismal systems", and "environmental information processing", all of which were also involved in cancer (microRNAs in cancer, choline metabolism in cancer, gastric cancer, breast cancer), signal transduction (mTOR, Hippo, sphingolipid, and phosphatidylinositol signaling), immune system (T cell receptor signaling pathway), etc. Detailed information is shown in Fig. 5D.

Discussion

Prostatitis seriously affects men's health, and the malignant development of prostate tissue cells may further transform into prostate cancer. Even though it is one of the most prevalent prostate disorders in the world, CNP is still debatable in terms of its genesis. The current knowledge on its pathogenesis mainly involves pathogen infection, inflammation, immunity, heredity, and oxidative stress.[30–32] However, accumulated evidence has indicated that TCM has amassed rich experience in clinical practice and achieved certain curative effects in the treatment of prostate diseases. Due to the disadvantages of poor water solubility and low bioavailability of artemisinin, DHA, an important derivative of artemisinin, exhibits better bioavailability and increased antimalarial effects compared to artemisinin. In addition, DHA also has anti-inflammatory and anti-tumor activity, among other pharmacological effects. Herein, we examined how DHA affected mice with prostatitis caused by the administration of prostate tissue and complete Freund's adjuvant. The EAP model is straightforward to construct and has a high success rate. The modeled

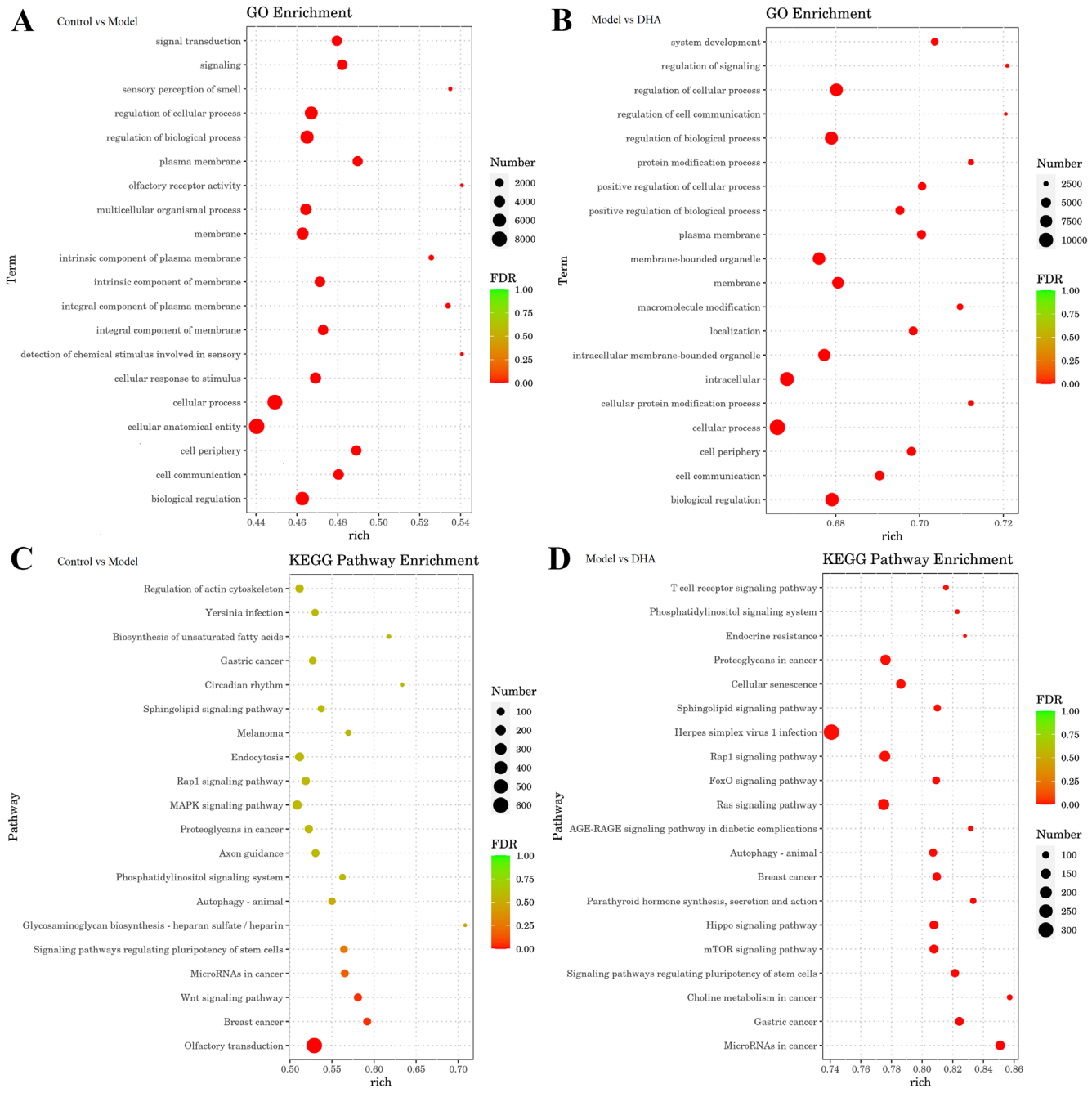

Fig. 5. Function and pathway analysis of the target genes of differentially expressed miRNAs (DEMs). A. Gene Ontology (GO) enrichment analysis between the control and model groups; B. GO enrichment analysis between the model and dihydroartemisinin (DHA) group; C. Kyoto Encyclopedia of Genes and Genomes (KEGG) enrichment analysis between the control and model group; D. KEGG enrichment analysis between the model and DHA group. The false discovery rate (FDR) value ranges from 0 to 1, with the values closer to 0 indicating a more substantial enrichment

CNP, which has been widely used, may cause a significant inflammatory response in the prostate gland with strong pathological specificity, prolonged model duration, and pathological changes similar to clinical manifestations. In this study, the results showed that DHA significantly improved CNP. Dihydroartemisinin reduced the frequency of pain responses, improved the epithelial cells and glandular ducts of the prostate tissue, reduced inflammatory infiltration, and decreased the prostate index. Simultaneously, DHA significantly reduced apoptosis and the inflammatory response in prostate tissue.

Previous investigations have demonstrated that cytokines and inflammation are key factors in the development of CNP.[33] When the prostate is stimulated, it produces a wide range of host defense and inflammatory factors.[34] The IL-1β is a critical pro-inflammatory factor that leads to the occurrence and persistence of inflammation. The release of caspase-1 induced by NOD-like receptor protein 3 (NLRP3) inflammasome and the downstream

cytokine IL-1β may be one of the pathogenic mechanisms of prostatitis.[35,36] The IL-6 is an important pro-inflammatory interleukin, and the level of IL-6 in CNP has been strongly correlated to the intensity of patients' clinical symptoms.[37] The IL-6 is a pleiotropic cytokine that regulates T cell migration and chronic immune responses and is strongly linked to prostate cell growth and death.[38] In addition, IL-6 may regulate the occurrence and development of CNP by regulating cellular autophagy.[39] The TNF-α is a major pro-inflammatory cytokine that is involved in the induction of inflammatory responses as well as the regulation of immune responses.[33] Furthermore, TNF-α can increase the production of cytokines, including IL-1, IL-6 and IL-8, by neutrophils and mononuclear macrophages, which stimulates the inflammatory cascade and exacerbates the inflammatory response.[40] In addition to inflammatory factors, MCP-1 is used as an inflammatory biomarker to identify the response of CNP patients to treatment.[38] Research has revealed that MCP-1 activates monocytes and macrophages and is involved in chemotaxis.[41] It promoted the production of pro-inflammatory cytokines, which in turn boosted the inflammatory response in the CNP pathological conditions. Our previous clinical study showed that reducing prostate inflammatory levels was effective in relieving urinary tract infections in prostate cancer patients.[42] In the current investigation, CNP had elevated levels of IL-1β, TNF-α and IL-6, while DHA markedly decreased these, as well as suppressed MCP-1 levels in prostate tissue. Therefore, DHA may be beneficial for preventing the development of CNP by downregulating inflammatory factors and inflammatory mediators.

Changes in miRNA expression profiles are currently the subject of substantial research in conditions like prostate cancer, but studies in CNP are still relatively sparse. We used small RNA sequencing and real-time PCR to evaluate and validate the abnormally expressed miRNAs in order to further clarify the mechanism underlying DHA's impact on the miRNA expression profile in CNP mice. Small RNA is a key regulator of biological processes, including the control of gene expression, biological maturation, metabolism, and the emergence of illness, and CNP pathogenesis is accompanied by abnormal miRNA expression.[43] We found 48 target gene miRNAs, indicating that DHA has a powerful role in altering prostate miRNA expression. The RNA sequencing results showed that 4 miRNAs (*miR-467a-5p*, *miR-467b-5p*, *miR-335-3p*, *miR-669c-5p*) were dramatically diminished in the model group and substantially elevated after DHA treatment. Meanwhile, 2 miRNAs (*miR-490-3p*, *miR-672-5p*) were elevated in the CNP mice and depressed after DHA treatment. Previous investigations have reported that *miR-467a-5p* reduced inflammation and elevated blood glucose and insulin levels to prevent insulin resistance.[44] The *miR-335-3p* was involved in regulating the inflammatory response in myocardial infarction, ulcerative colitis and Parkinson's disease.[45–47] The *miR-669c-5p* has been reported to be differentially expressed in mouse spermatocyte-derived GC-2 cells and may affect male reproductive function.[48] The *miR-490-3-p* was elevated in the reproductive organs of male rats induced by a high cholesterol diet,[49] while *miR-672-5p* was shown to be altered in the kidney of urolithiasis rats.[50] Therefore, these genes have the potential to become novel biomarkers and therapeutic targets for CNP. In this study, we performed a preliminary investigation of DEMs in CNP, and the relationship of these miRNAs with inflammatory, immune, metabolic and other signaling pathways and their mechanisms need to be further examined.

The KEGG pathway analysis of miRNA expression profile in the CNP mice revealed several signaling pathways related to the pathogenesis of CNP. These included the phosphatidylinositol signaling system, Wnt, MAPK, Rap1, and sphingolipid signaling pathway, and there is a clear correlation between some signaling pathways. However, the role of miRNAs and related signal transduction pathways in CNP occurrence and development needs further investigation. Of note, the development of DHA therapy for CNP involves several signaling pathways, including the mTOR, Hippo, sphingolipid, phosphatidylinositol, and T cell receptor signaling pathways. As expected, we found that all these pathways are involved in inflammatory and immune responses, suggesting a key regulatory role for inflammation and the immune system in initiating and progressing CNP. For example, Akt-mTOR could modulate the immune response and prevent Th17 cell over-activation in order to improve chronic prostatitis and chronic pelvic pain syndrome (CP/CPPS).[51] Jiedu Huoxue decoction was found to inhibit apoptosis and activate the Wnt/GSK-3β/β-catenin signaling pathway to treat CP/CPPS.[52] In addition, inflammatory factors could reduce CP/CPPS by downregulating NF-κB and JNK/MAPK pathway to alleviate prostatitis pain.[53] In this study, DHA has demonstrated a powerful therapeutic effect for CNP. However, the role of DHA in the CNP by regulating miRNA profiles acting on inflammatory, immune and apoptotic pathways deserves further exploration.

Limitations

In this study, we screened some DEMs by transcriptomics, but the role of these miRNAs in prostatitis mice remains to be further investigated. Meanwhile, we found that inflammation and the immune system play a key regulatory role in the CNP, but the exact mechanism still needs to be examined.

Conclusions

This study explored the effectiveness and mechanism of DHA in the treatment of CNP. We found considerable improvement in the pathogenic condition following

DHA administration in a CNP mouse model. The development of biomarkers associated with CNP will be based on the detection of miRNA expression profiles in prostate tissues, which will aid in the early detection, diagnosis and treatment of CNP diseases. This work added to the body of knowledge on the mechanism of DHA in the treatment of CNP and may offer a fresh approach to its prevention and management.

Supplementary data

The Supplementary materials are available at https://zenodo.org/record/8327619. The package contains the following files:

Supplementary Table 1. The normality test and statistical analysis of multiple dependent variable of Fig. 1.

Supplementary Table 2. The normality test and statistical analysis of multiple dependent variable of Fig. 2.

Supplementary Table 3. The normality test and statistical analysis of multiple dependent variable of Fig. 4.

ORCID iDs

Jie Hu https://orcid.org/0009-0009-5906-0837
Yan Zhou https://orcid.org/0009-0007-1095-4739
Junhao Wang https://orcid.org/0009-0002-6243-8908
Jianpeng Han https://orcid.org/0009-0002-4045-2039
Jianyong Feng https://orcid.org/0009-0003-2306-6416
Wenbin Chen https://orcid.org/0009-0008-1601-6935
Kuo Guo https://orcid.org/0009-0006-9360-5464
Yongzhang Li https://orcid.org/0000-0002-6249-5198

References

1. Fuentes IM, Jones BM, Brake AD, et al. Voluntary wheel running improves outcomes in an early life stress-induced model of urologic chronic pelvic pain syndrome in male mice. *Pain*. 2021;162(6):1681–1691. doi:10.1097/j.pain.0000000000002178
2. Liu H, Wang Z, Xie Q, et al. Ningmitai capsules have anti-inflammatory and pain-relieving effects in the chronic prostatitis/chronic pelvic pain syndrome mouse model through systemic immunity. *Front Pharmacol*. 2022;13:949316. doi:10.3389/fphar.2022.949316
3. Zang L, Tian F, Yao Y, et al. Qianliexin capsule exerts anti-inflammatory activity in chronic non-bacterial prostatitis and benign prostatic hyperplasia via NF-κB and inflammasome. *J Cell Mol Med*. 2021;25(12):5753–5768. doi:10.1111/jcmm.16599
4. Zeng F, Chen H, Yang J, et al. Development and validation of an animal model of prostate inflammation-induced chronic pelvic pain: Evaluating from inflammation of the prostate to pain behavioral modifications. *PLoS One*. 2014;9(5):e96824. doi:10.1371/journal.pone.0096824
5. Pontari MA. Etiology of chronic prostatitis/chronic pelvic pain syndrome: Psychoimmunoneurendocrine dysfunction (PINE syndrome) or just a really bad infection? *World J Urol*. 2013;31(4):725–732. doi:10.1007/s00345-013-1061-z
6. Zhang Y, Li X, Zhou K, et al. Influence of experimental autoimmune prostatitis on sexual function and the anti-inflammatory efficacy of celecoxib in a rat model. *Front Immunol*. 2020;11:574212. doi:10.3389/fimmu.2020.574212
7. Lee G. Chronic prostatitis: A possible cause of hematospermia. *World J Mens Health*. 2015;33(2):103. doi:10.5534/wjmh.2015.33.2.103
8. Almeer RS, Muhammad NAE, Othman MS, Aref AM, Elgamal B, Moneim AEA. The potential protective effect of orange peel and selenium against 17β-estradiol-induced chronic non-bacterial prostatitis in rats. *Anticancer Agents Med Chem*. 2020;20(9):1061–1071. doi:10.2174/1871520620666200331102609
9. Isik A, Wysocki AP, Memiş U, Sezgin E, Yezhikova A, Islambekov Y. Factors associated with the occurrence and healing of umbilical pilonidal sinus: A rare clinical entity. *Adv Skin Wound Care*. 2022;35(8):1–4. doi:10.1097/01.ASW.0000833608.27136.d1
10. Isik A, Soran A, Grasi A, Barry N, Sezgin E. Lymphedema after sentinel lymph node biopsy: Who is at risk? *Lymph Res Biol*. 2022;20(2):160–163. doi:10.1089/lrb.2020.0093
11. Doiron RC, Nickel JC. Management of chronic prostatitis/chronic pelvic pain syndrome. *Can Urol Assoc J*. 2018;12(6 Suppl 3):S161–S163. doi:10.5489/cuaj.5325
12. Holt JD, Garrett WA, McCurry TK, Teichman JMH. Common questions about chronic prostatitis. *Am Fam Physician*. 2016;93(4):290–296. PMID:26926816.
13. Yi J, Pan J, Zhang S, et al. Improvement of chronic non-bacterial prostatitis by Jiedu Huoxue decoction through inhibiting TGF-β/SMAD signaling pathway. *Biomed Pharmacother*. 2022;152:113193. doi:10.1016/j.biopha.2022.113193
14. Chen JX, Hu LS. Traditional Chinese Medicine for the treatment of chronic prostatitis in China: A systematic review and meta-analysis. *J Altern Complement Med*. 2006;12(8):763–769. doi:10.1089/acm.2006.12.763
15. Dai X, Zhang X, Chen W, et al. Dihydroartemisinin: A potential natural anticancer drug. *Int J Biol Sci*. 2021;17(2):603–622. doi:10.7150/ijbs.50364
16. Klayman DL. Qinghaosu (artemisinin): An antimalarial drug from China. *Science*. 1985;228(4703):1049–1055. doi:10.1126/science.3887571
17. Luo XD, Shen CC. The chemistry, pharmacology, and clinical applications of Qinghaosu (artemisinin) and its derivatives. *Med Res Rev*. 1987;7(1):29–52. doi:10.1002/med.2610070103
18. Van Agtmael M. Artemisinin drugs in the treatment of malaria: From medicinal herb to registered medication. *Trends Pharmacol Sci*. 1999;20(5):199–205. doi:10.1016/S0165-6147(99)01302-4
19. Yu R, Jin G, Fujimoto M. Dihydroartemisinin: A potential drug for the treatment of malignancies and inflammatory diseases. *Front Oncol*. 2021;11:722331. doi:10.3389/fonc.2021.722331
20. Gutman J, Kovacs S, Dorsey G, Stergachis A, Ter Kuile FO. Safety, tolerability, and efficacy of repeated doses of dihydroartemisinin-piperaquine for prevention and treatment of malaria: A systematic review and meta-analysis. *Lancet Infect Dis*. 2017;17(2):184–193. doi:10.1016/S1473-3099(16)30378-4
21. Ho WE, Peh HY, Chan TK, Wong WSF. Artemisinins: Pharmacological actions beyond anti-malarial. *Pharmacol Ther*. 2014;142(1):126–139. doi:10.1016/j.pharmthera.2013.12.001
22. Li WD, Dong YY, Tu YY, Lin ZB. Dihydroarteannuin ameliorates lupus symptom of BXSB mice by inhibiting production of TNF-alpha and blocking the signaling pathway NF-kappa B translocation. *Int Immunopharmacol*. 2006;6(8):1243–1250. doi:10.1016/j.intimp.2006.03.004
23. Yang B, Gao X, Sun Y, et al. Dihydroartemisinin alleviates high glucose-induced vascular smooth muscle cells proliferation and inflammation by depressing the miR-376b-3p/KLF15 pathway. *Biochem Biophys Res Commun*. 2020;530(3):574–580. doi:10.1016/j.bbrc.2020.07.095
24. Zhou Y, Wang JH, Han JP, et al. Dihydroartemisinin ameliorates chronic nonbacterial prostatitis and epithelial cellular inflammation by blocking the E2F7/HIF1α pathway. *Inflamm Res*. 2022;71(4):449–460. doi:10.1007/s00011-022-01544-8
25. Chen H, Zhang Z. A miRNA-driven inference model to construct potential drug-disease associations for drug repositioning. *Biomed Res Int*. 2015;2015:406463. doi:10.1155/2015/406463
26. Gee LE, Chen N, Ramirez-Zamora A, Shin DS, Pilitsis JG. The effects of subthalamic deep brain stimulation on mechanical and thermal thresholds in 6OHDA-lesioned rats. *Eur J Neurosci*. 2015;42(4):2061–2069. doi:10.1111/ejn.12992
27. Schaeffer EM. Re: Th1–Th17 cells contribute to the development of uropathogenic *Escherichia coli*-induced chronic pelvic pain. *J Urol*. 2014;191(6):1808–1809. doi:10.1016/j.juro.2014.03.029
28. Choi YJ, Lee JI, Fan M, et al. Metabolomic analysis of *Morus cultivar* root extracts and their ameliorative effect on testosterone-induced prostate enlargement in Sprague Dawley rats. *Int J Mol Sci*. 2020;21(4):1435. doi:10.3390/ijms21041435
29. Wang YL, Zhang Y, Cai DS. Hepatoprotective effects of sevoflurane against hepatic ischemia–reperfusion injury by regulating microRNA-124-3p-mediated TRAF3/CREB axis. *Cell Death Discov*. 2022;8(1):105. doi:10.1038/s41420-021-00784-7

30. Zhang M, Liu Y, Chen J, et al. Single-cell multi-omics analysis presents the landscape of peripheral blood T-cell subsets in human chronic prostatitis/chronic pelvic pain syndrome. *J Cell Mol Med*. 2020; 24(23):14099–14109. doi:10.1111/jcmm.16021
31. Sfanos KS, De Marzo AM. Prostate cancer and inflammation: The evidence. *Histopathology*. 2012;60(1):199–215. doi:10.1111/j.1365-2559.2011.04033.x
32. Wang GC, Huang TR, Hu YY, et al. Corpus cavernosum smooth muscle cell dysfunction and phenotype transformation are related to erectile dysfunction in prostatitis rats with chronic prostatitis/chronic pelvic pain syndrome. *J Inflamm*. 2020;17(1):2. doi:10.1186/s12950-019-0233-z
33. Kang SW, Park JH, Seok H, et al. The effects of Korea Red Ginseng on inflammatory cytokines and apoptosis in rat model with chronic nonbacterial prostatitis. *Biomed Res Int*. 2019;2019:2462561. doi:10.1155/2019/2462561
34. Castiglione R, Salemi M, Vicari LO, Vicari E. Relationship of semen hyperviscosity with IL-6, TNF-α, IL-10 and ROS production in seminal plasma of infertile patients with prostatitis and prostato-vesiculitis. *Andrologia*. 2014;46(10):1148–1155. doi:10.1111/and.12207
35. Zhou R, Yazdi AS, Menu P, Tschopp J. A role for mitochondria in NLRP3 inflammasome activation. *Nature*. 2011;469(7329):221–225. doi:10.1038/nature09663
36. McGettrick AF, O'Neill LAJ. How metabolism generates signals during innate immunity and inflammation. *J Biol Chem*. 2013;288(32): 22893–22898. doi:10.1074/jbc.R113.486464
37. Stancik I, Plas E, Juza J, Pflüger H. Effect of antibiotic therapy on interleukin-6 in fresh semen and postmasturbation urine samples of patients with chronic prostatitis/chronic pelvic pain syndrome. *Urology*. 2008; 72(2):336–339. doi:10.1016/j.urology.2008.04.005
38. Xiong Y, Zhou L, Qiu X, Miao C. Anti-inflammatory and anti-hyperplastic effect of Bazhengsan in a male rat model of chronic nonbacterial prostatitis. *J Pharmacol Sci*. 2019;139(3):201–208. doi:10.1016/j.jphs.2019.01.007
39. Santarelli R, Gonnella R, Di Giovenale G, et al. STAT3 activation by KSHV correlates with IL-10, IL-6 and IL-23 release and an autophagic block in dendritic cells. *Sci Rep*. 2014;4(1):4241. doi:10.1038/srep04241
40. Jang TL, Schaeffer AJ. The role of cytokines in prostatitis. *World J Urol*. 2003;21(2):95–99. doi:10.1007/s00345-003-0335-2
41. Singh S, Anshita D, Ravichandiran V. MCP-1: Function, regulation, and involvement in disease. *Int Immunopharmacol*. 2021;101:107598. doi:10.1016/j.intimp.2021.107598
42. Wang J, Han J, Feng J, et al. Effect of Bushen Huoxue decoction combined with moxibustion on inflammation and urinary symptoms in patients with prostate cancer. *Am J Transl Res*. 2022;14(12):8991–9000.
43. Chen Y, Chen S, Zhang J, et al. Expression profile of microRNAs in expressed prostatic secretion of healthy men and patients with IIIA chronic prostatitis/chronic pelvic pain syndrome. *Oncotarget*. 2018; 9(15):12186–12200. doi:10.18632/oncotarget.24069
44. Gajeton J, Krukovets I, Yendamuri R, et al. miR-467 regulates inflammation and blood insulin and glucose. *J Cell Mol Med*. 2021;25(5): 2549–2562. doi:10.1111/jcmm.16224
45. Oliveira SR, Dionísio PA, Correia Guedes L, et al. Circulating inflammatory miRNAs associated with Parkinson's disease pathophysiology. *Biomolecules*. 2020;10(6):945. doi:10.3390/biom10060945
46. Ranjha R, Aggarwal S, Bopanna S, Ahuja V, Paul J. Site-specific microRNA expression may lead to different subtypes in ulcerative colitis. *PLoS One*. 2015;10(11):e0142869. doi:10.1371/journal.pone.0142869
47. Bakhshi A, Khani M, Alipour Parsa S, et al. Investigating the expression level of miR-17-3p, miR-101-3p, miR-335-3p, and miR-296-3p in the peripheral blood of patients with acute myocardial infarction [published online ahead of print on May 24, 2023]. *Mol Cell Biochem*. 2023. doi:10.1007/s11010-023-04766-4
48. Liu Y, Liu WB, Liu KJ, et al. Extremely low-frequency electromagnetic fields affect the miRNA-mediated regulation of signaling pathways in the GC-2 cell line. *PLoS ONE*. 2015;10(10):e0139949. doi:10.1371/journal.pone.0139949
49. Lim W, Bae H, Song G. Differential expression of apolipoprotein D in male reproductive system of rats by high-fat diet. *Andrology*. 2016; 4(6):1115–1122. doi:10.1111/andr.12250
50. Cao Y, Gao X, Yang Y, Ye Z, Wang E, Dong Z. Changing expression profiles of long non-coding RNAs, mRNAs and circular RNAs in ethylene glycol-induced kidney calculi rats. *BMC Genomics*. 2018;19(1):660. doi:10.1186/s12864-018-5052-8
51. Zhan C, Chen J, Chen J, et al. CaMK4-dependent phosphorylation of Akt/mTOR underlies Th17 excessive activation in experimental autoimmune prostatitis. *FASEB J*. 2020;34(10):14006–14023. doi:10.1096/fj.201902910RRR
52. Yi J, Pan J, Zhang S, et al. Jiedu Huoxue decoction improves chronic abacterial prostatitis/chronic pelvic pain syndrome through activating Wnt/GSKβ/β-catenin signaling pathway and alleviating apoptosis. *Biomed Pharmacother*. 2022;149:112830. doi:10.1016/j.biopha.2022.112830
53. Liu H, Zhu X, Cao X, et al. IL-1β-primed mesenchymal stromal cells exert enhanced therapeutic effects to alleviate chronic prostatitis/chronic pelvic pain syndrome through systemic immunity. *Stem Cell Res Ther*. 2021;12(1):514. doi:10.1186/s13287-021-02579-0